THE JOURNAL OF BIOLOGICAL CHEMISTRY VOL. 283, NO. 19, pp. 13357–13369, May 9, 2008

Male Germ Cells Require Polyenoic Sphingolipids with Complex Glycosylation for Completion of Meiosis

A LINK TO CERAMIDE SYNTHASE-3[*] [S]

Received for publication, February 1, 2008 Published, JBC Papers in Press, February 27, 2008, DOI 10.1074/jbc.M800870200

Mariona Rabionet[‡], Aarnoud C. van der Spoel[§1], Chia-Chen Chuang[§], Benita von Tümpling-Radosta[‡], Manja Litjens[§2], Diane Bouwmeester[§3], Christina C. Hellbusch[¶], Christian Körner[¶], Herbert Wiegandt[‡], Karin Gorgas[‖], Frances M. Platt[§], Hermann-Josef Gröne[‡], and Roger Sandhoff[‡4]

From the [‡]Department of Cellular and Molecular Pathology, German Cancer Research Center, INF 280, 69120 Heidelberg, Germany, the [§]Department of Pharmacology, University of Oxford, Mansfield Road, Oxford OX1 3QT, United Kingdom, the [¶]Department of Pediatrics, Division of Inborn Metabolic Diseases, University Children's Hospital, INF 153, 69120 Heidelberg, Germany, and the [‖]Department of Anatomy and Cell Biology II, University of Heidelberg, INF 307, 69120 Heidelberg, Germany

Previously, it was found that a novel class of neutral fucosylated glycosphingolipids (GSLs) is required for male fertility. These lipids contain very long-chain (C26–C32) polyunsaturated (4–6 double bonds) fatty acid residues (VLC-PUFAs). To assess the role of these complex GSLs in spermatogenesis, we have now investigated with which of the testicular cell types these lipids are associated. During postnatal development, complex glycosylated and simple VLC-PUFA sphingolipids were first detectable at day 15, when the most advanced germ cells are pachytene spermatocytes. Their synthesis is most likely driven by ceramide synthase-3. This enzyme is encoded by the *Cers3*/*Lass3* gene (longevity assurance genes), and out of six members of this gene family, only *Cers3* mRNA expression was limited to germ cells, where it was up-regulated more than 700-fold during postnatal testicular maturation. Increasing levels of neutral complex VLC-PUFA GSLs also correlated with the progression of spermatogenesis in a series of male sterile mutants with arrests at different stages of spermatogenesis. Remarkably, fucosylation of the complex VLC-PUFA GSLs was not essential for spermatogenesis, as fucosylation-deficient mice produced nonfucosylated versions of the complex testicular VLC-PUFA GSLs, had complete spermatogenesis, and were fertile. Nevertheless, sterile *Galgt1*$^{-/-}$ mice, with a defective meiotic cytokinesis and a subsequent block in spermiogenesis, lacked complex but contained simple VLC-PUFA GSLs, as well as VLC-PUFA ceramides and sphingomyelins, indicating that the latter lipids are not sufficient for completion of spermatogenesis. Thus, our data imply that both glycans and the particular acyl chains of germinal sphingolipids are relevant for proper completion of meiosis.

The testis is composed of two functional compartments as follows: (i) the seminiferous tubules, containing developing germ cells and supporting Sertoli cells, and (ii) the steroidogenic Leydig cells in the interstitium (Fig. 1*A*) (1, 2). In mature testis, the seminiferous tubules are separated by a blood-testis barrier (BTB)[5] into a basal and an adluminal compartment. Tight junctions contribute to the establishment of the BTB, which is made up of adjacent Sertoli cells and physically segregates post-meiotic germ cells from nutrients and biomolecules in the systemic circulation (3, 4).

The development of the male germ cells, taking place within the seminiferous tubules, is a complex and highly regulated process (2). During spermatogenesis, testicular stem cells (undifferentiated spermatogonia) give rise to a lineage of cells that multiply by mitosis (proliferative spermatogonia). These cells differentiate to go through the meiotic division (spermatocytes) and become haploid germ cells (spermatids), which transform into spermatozoa. It is during the meiotic prophase that leptotene spermatocytes transit the BTB. The post-meiotic development (spermiogenesis) involves a dramatic change of nuclear shape, chromatin condensation, the loss of most cell organelles, and the formation of specialized structures, including a flagellum, an acrosome, and a mitochondrial sheath.

* This work was supported, in whole or in part, by National Institutes of Health Grant 1 U01 HD45861 (to A. C. S. and F. M. P.). This work was also supported by the German Research Foundation Grants SA 1721/1-1 and GO 432/2-1, Schering AG (to C. C. C.), and the Oxford Glycobiology Institute endowment. The costs of publication of this article were defrayed in part by the payment of page charges. This article must therefore be hereby marked "*advertisement*" in accordance with 18 U.S.C. Section 1734 solely to indicate this fact.

[S] The on-line version of this article (available at http://www.jbc.org) contains supplemental Experimental Procedures, additional references, Table 1, and Figs. 1–8.

[1] To whom correspondence may be addressed. E-mail: aarnoud.vanderspoel@pharm.ox.ac.uk.

[2] Present address: Dept. of Molecular Cell Biology and Immunology, Free University Medical Center, 1081 BT Amsterdam, The Netherlands.

[3] Present address: Dept. of Physiological Chemistry, University Medical Center Utrecht, 3584 CG Utrecht, The Netherlands.

[4] To whom correspondence may be addressed. E-mail: r.sandhoff@dkfz-heidelberg.de.

[5] The abbreviations used are: BTB, blood-testis barrier; Bax, BCL2 associated X-protein; BL6, C57BL/6 mouse strain; Cer, ceramide; CerS1–6, ceramide synthase 1–6; CREM, cyclic AMP-responsive element modulator; FGSLs, fucosylated GSLs; GSLs, glycosphingolipids; GlcCer, glucosylceramide; P5–35, postnatal day 5–35; PUSLs, polyunsaturated sphingolipids; *Siat9*/*St3gal5*, β-galactoside α-2,3-sialyltransferase 5 (GM3-synthase); SM, sphingomyelin; SM4g, seminolipid (GalEAG I^3-sulfate); Sxr, sex-reversed factor, which is an extra copy of the testis-determining region of the mouse Y chromosome but without the Y chromosomal gene required for transplantation H-Y antigen expression; VLC-PUFA, very long-chain polyunsaturated fatty acids; HPLC, high pressure liquid chromatography; qRT, quantitative real time PCR; GAPDH, glyceraldehyde-3-phosphate dehydrogenase; PUSL, VLC-PUFA sphingolipids. The glycolipid nomenclature described by Svennerholm (46) and recommended by the IUPAC (*Pure Appl. Chem.* (1997) **69,** 2475–2487).

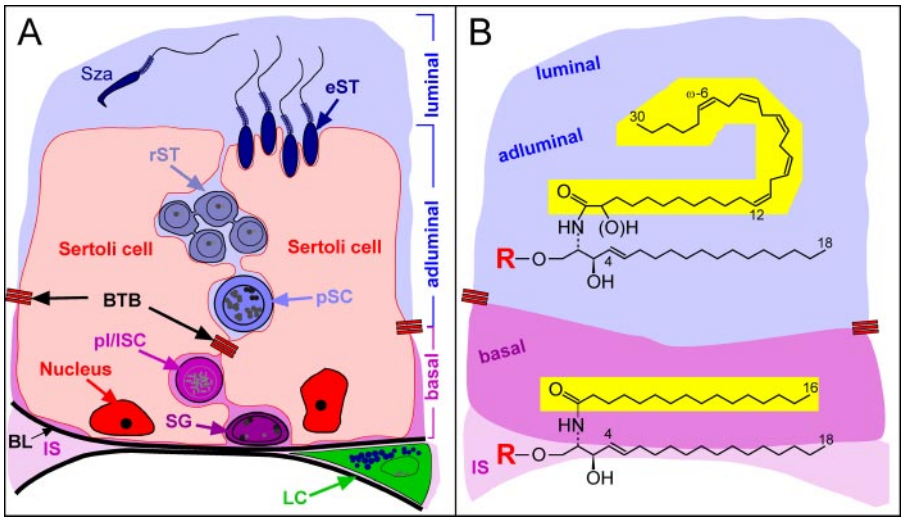

FIGURE 1. *A,* schematic drawing of spermatogenesis within the seminiferous epithelium. *B,* testicular sphingolipid structures, the ceramide moiety. *A,* supporting Sertoli cells (*red*) adhere to the basal lamina (*BL*) and develop in addition to the BTB several junctions and specialized contacts to germ cells during all differentiation stages. Spermatogonia (*SG*) are also adherent to the basal lamina. Spermatogonia type A divide and develop into spermatogonia type B, which enter meiotic prophase and differentiate into primary spermatocytes (*SC,* preleptotene (*plSC*) → leptotene (*lSC*) → zygotene → pachytene (*pSC*)). Pachytene spermatocytes have traversed the BTB and complete meiosis within the adluminal compartment. Four round haploid spermatids arise from one pachytene spermatocyte and undergo spermiogenesis in 16 steps, including elongated spermatids (*eST*). Spermatozoa (*Sza*) are finally released into the lumen. Testosterone producing Leydig cells (*LC*) are located in the interstitium (*IS*) between adjacent tubules. *B,* ceramide moieties of testicular sphingolipids consist of a d18:1-sphingosine base to which a fatty acid is linked through an amide bond. In case of interstitial cells, Sertoli cells and germ cells of the basal compartment of these fatty acid moieties are of long-chain and saturated (mainly palmitic acid), whereas in the case of adluminal germ cells and spermatozoa, they are of very long-chain (C28–32) and polyunsaturated (5–6 double bonds). The sphingolipid head group (*R*) may be ceramide (*H*), phosphorylcholine (sphingomyelin), Glc, Lac, Gb_{3-5}, or a complex ganglioside oligosaccharide in case of somatic cells (*e.g.* Sertoli, Leydig cells) and ceramide, phosphorylcholine, Glc, Lac, and acidic or neutral fucosylated complex ganglio series oligosaccharides in case of germ cells.

In mice, spermatogenesis is dependent on two types of glycolipids, seminolipid, a sulfated galactoglycerolipid (5–7), and glycosphingolipids (GSLs) (8, 9). GSLs are amphipathic cell membrane molecules present on the extracellular leaflet of the plasma membrane lipid bilayers and on topologically equivalent membrane sides of endocytotic and exocytotic organelles (10). They modulate membrane properties and receptors (11, 12) or ion channel functions (6, 13, 14).

Loss of ganglio-series GSLs by systemic deletion of the GalNAc transferase (*Galgt1*$^{-/-}$) (Fig. 2) renders male mice sterile. Their spermatogenesis, the transformation of diploid spermatogonial stem cells into haploid spermatozoa, abrogates at the stage of haploid spermatid formation. Spermatogonial stem cell division, proliferation, and differentiation into preleptotene and leptotene spermatocytes appears unchanged. However, after adluminal completion of meiotic karyokinesis, haploid round spermatids aggregate in multinuclear giant cells. Spermiogenesis does not take place in *Galgt1*$^{-/-}$ mice (8, 15).

Recently, we performed a detailed analysis of GSLs in mouse testis revealing the presence of more than 13 complex neutral and acidic GSLs. Of these GSLs a class of eight fucosylated GSLs (FGSLs) was discovered to contain polyenoic (4–6 double bonds) very long-chain fatty acid residues (C26–C32) in their ceramide moieties (Fig. 2) (9). These structures were also found to be present in rat testis (9). Comparison of infertile *Galgt1*$^{-/-}$ and fertile *Siat9*$^{-/-}$ mice, lacking different subsets of GSLs, linked the absence of neutral polyenoic FGSLs to the spermatogenic arrest of meiosis in *Galgt1*$^{-/-}$ mice suggesting an essential role of polyenoic FGSLs in meiotic and post-meiotic membrane processes (9). Three of the eight FGSLs could be linked to germ cells by immunocytochemistry, with the other five FGSLs still remaining to be localized (9). Two features distinguish the polyenoic FGSLs from conventional GSLs as follows: (i) their fucosylation and (ii) their fatty acid tail being mainly of very long chain and polyenoic. Both structural features could be essential for proper spermatogenesis, which has still to be clarified. In this study we present the following: (i) we classify and localize fucosylated GSLs to different germ cell classes according to their charge; (ii) we demonstrate that polyenoic very long-chain fatty acid-containing sphingolipids in general (FGSLs, GSLs, ceramides, and sphingomyelins) are restricted to germ cells and are expressed in a differentiation stage-specific manner (Fig. 1*B*); (iii) we link the synthesis of polyenoic VLCFA sphingolipids to the expression of one of six potential (dihydro)ceramide synthases; and (iv) we show the dispensability of sphingolipid fucosylation for the generation of functional spermatozoa.

EXPERIMENTAL PROCEDURES

Mice—Postnatal lipid analysis (P5–P35) was performed from testes of C57BL/6 mice obtained from Charles River WIGA (Deutschland) GmbH, Sulzfeld, Germany. The following mutant mice were analyzed: *Slc35c1*$^{-/-}$ (16), *Galgt1*$^{-/-}$ (15), and *Kit*$^{W\text{-}v}$/*Kit*^{W} (Jax Stock number 100410; 6–8 weeks old), *mshi/mshi* (*mshi* indicates male sterility and histoincompatibility; number 002169), and *bax*$^{-/-}$ (number 002994; 6–8 weeks old) were obtained from The Jackson Laboratory, Bar Harbor, ME. Testes from *CREM*$^{-/-}$ mice (8–16 weeks old) were provided by Paolo Sassone-Corsi (Institut de Génétique et de Biologie Moléculaire et Cellulaire, Strasbourg, France), and *XXSxr*^{b} mice (8–12 weeks old; where XXSxr^{b} indicates male mice with two copies of the X chromosome that contains the Sxr^{b} region) were provided by Paul Burgoyne (MRC National Institute for Medical Research, London, UK).

GSL Extraction for TLC and ESI-MS/MS Analysis—GSLs were extracted from testes according to Ref. 17. In brief, tissue was homogenized on ice, lyophilized, and extracted twice with dry acetone. The residual pellet then was extracted twice with chloroform/methanol/water (C/M/W) (10:10:1) and with C/M/W (30:60:8). The combined C/M/W extracts were treated with 0.1 M methanolic KOH for 2 h at 37 °C, neutralized with acetic acid, and desalted with RP-18 column chromatography. Finally, neutral and acidic sphingo-

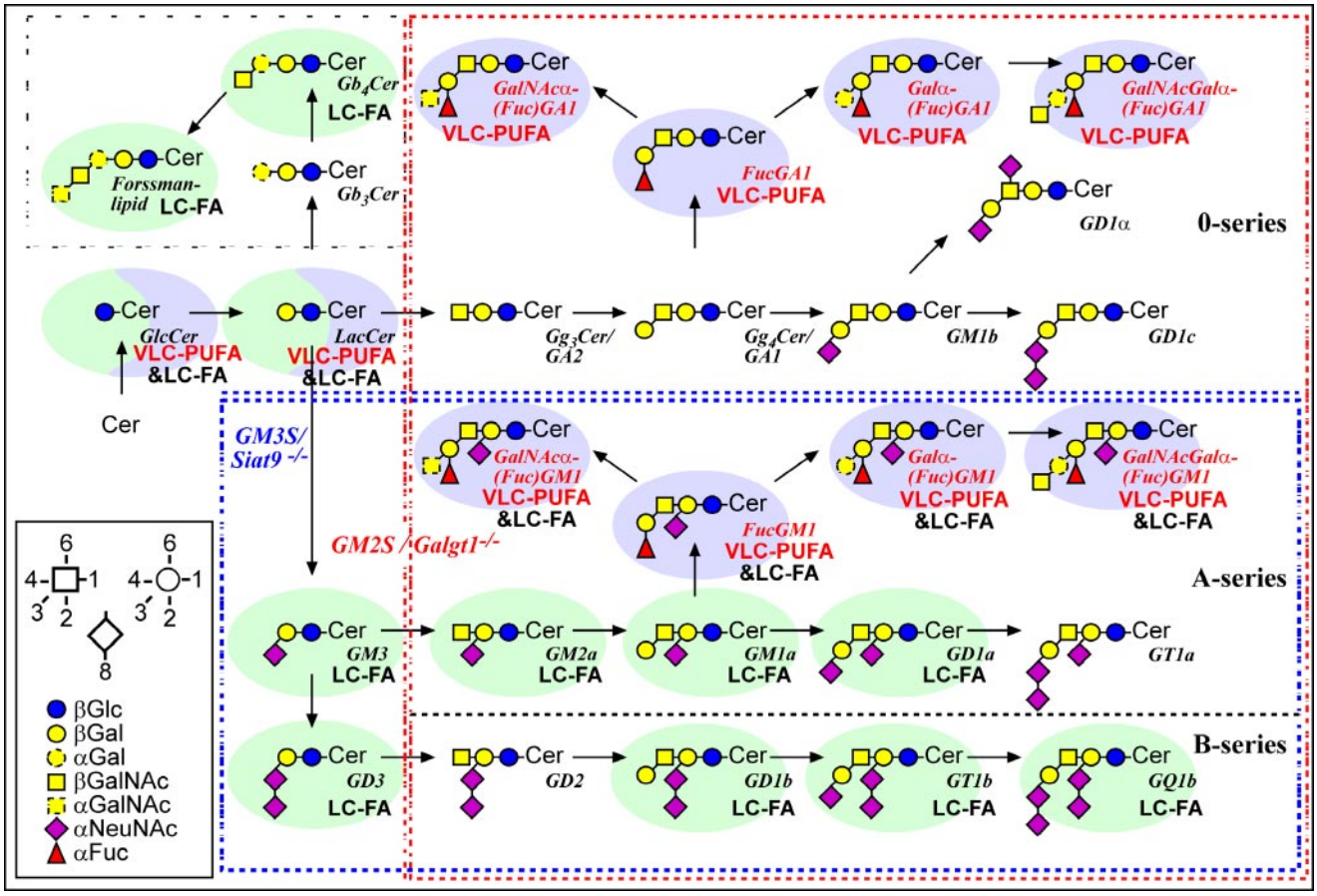

FIGURE 2. **Major pathways of testicular GSLs from ganglio- and globo-series.** The scheme is a modification from Ref. 9. Genes of enzymes deleted in mutant mice are indicated in color: *red*, *Galgt1* (GM2/GD2 synthase); *blue*, *Siat9* (GM3 synthase). GSLs depending on the presence of either GM2/GD2 synthase or GM3 synthase are bordered with a *dashed frame* of corresponding color. GSLs found in somatic cells are shaded with a *light green ellipse*, and those found in germ cells with a *light blue ellipse*. GSLs labeled with "*VLC-PUFA*" are with very long-chain polyunsaturated fatty acid moieties, and those labeled with "*LC-FA*" are with long-chain fatty acid moieties. Minor pathways caused by possible isoenzymes are not included.

lipids were separated on DEAE A-25 columns, and both were desalted again using RP-18 columns.

TLC Analysis—TLC analysis was performed according to Ref. 17. TLCs were developed with the solvent system $CHCl_3$, CH_3OH, 0.2% aqueous $CaCl_2$ = 60:35:8. Staining was performed with orcinol/sulfuric acid.

Nano-electrospray Ionization-Tandem Mass Spectrometry—Analysis was performed with a triple quadrupole instrument (VG Micromass (Cheshire, UK) model Quattro II) equipped with a nano-electrospray source and gold-sputtered capillaries as described (17). Parameters for cone voltage and collision energy of the different scan modes were used, and quantification of sphingolipids was performed according to previous publications (9, 17–19).

HPLC Analysis of GSLs—Extracted GSLs were digested with ceramidase, and the sugar moiety was purified and covalently linked to a fluorophore (anthranilic acid). The fluorescent sugar moieties then were separated and quantified using HPLC as described previously (20).

Histology—Serial semithin Epon sections (0.5–1 μm in thickness) were carried out as described previously (21). In brief, mice were anesthetized by a combination of ketamine and xylazine and subsequently perfused via either the left ventricle or the abdominal aorta. The fixative used for perfusion contained 1.5% paraformaldehyde, 1.5% glutaraldehyde, 2.5% polyvinylpyrrolidone dissolved in 0.1 M phosphate-buffered saline, pH 7.4. Organs were removed and 80–200 μm thick sections prepared by using a Dosaka microslicer. The sections were postfixed with 1.5% osmium ferrocyanide followed by 1.5% buffered osmium tetroxide. The samples were then stained *en bloc* with 1% uranyl acetate and processed for Epon embedding. Serial semithin sections (0.5–1 μm) were stained with a modified Richardson solution (methylene blue-Azur II).

Quantitative RT-PCR—Total mRNAs from juvenile and pubertal testes were isolated according to Chomczynski *et al.* (22). Testicular mRNAs from mutant/genetically modified mice were extracted using TRIzol reagent (Invitrogen) following the manufacturer's instructions. RNA quality was characterized using an RNA6000 Nanochip (Agilent Technologies, Waldbronn, Germany). Isolated mRNA was digested with TURBO DNA-free™ kit (Ambion) to remove DNA contamination. Double-stranded cDNA was synthesized using the SuperScript™ double-stranded cDNA synthesis kit (Invitrogen) as described by the manufacturer. For quantification of cDNA, real time PCR was performed by LightCycler® (System 2.0, Roche Diagnostics) using LightCycler-FastStart DNA MasterSYBR Green I kit (Roche Diagnostics) as described (23). Melting curves were performed to evaluate the integrity of the

TABLE 1
Primers used for qRT-PCR

Gene	Primer	Primer sequence	Product size
			bp
Gapdh	Forward	5′-ACT CCC ACT CTT CCA CCT TC-3′	156
	Reverse	5′-GGT CCA GGG TTT CTT ACT CC-3′	
Cers1	Forward	5′-TGA CTG GTC AGA TGC GTG A-3′	93
	Reverse	5′-TCA GTG GCT TCT CGG CTT T-3′	
Cers2	Forward	5′-TCA TCA TCA CTC GGC TGG T-3′	90
	Reverse	5′-AGC CAA AGA AGG CAG GGT A-3′	
Cers3	Forward	5′-ATC TCG AGC CCT TCT TCT CC-3′	128
	Reverse	5′-CTG GAC GTT CTG CGT GAA T-3′	
Cers4	Forward	5′-TGC GCA TGC TCT ACA GTT TC-3′	132
	Reverse	5′-CTC GAG CCA TCC CAT TCT T-3′	
Cers5	Forward	5′-TCC ATG CCA TCT GGT CCT A-3′	147
	Reverse	5′-TGC TGC CAG AGA GGT TGT T-3′	
Cers6	Forward	5′-GGG TTG AAC TGC TTC TGG TC-3′	138
	Reverse	5′-TTT CTT CCC TGG AGG CTC T-3′	

products. Relative expression of the *Cers/Lass* family genes was determined using the comparative *CT* method, normalizing relative values to the expression of GAPDH as a housekeeping gene (24). The primer sequences for target genes are listed in Table 1.

RESULTS

Seminiferous Tubules of $Kit^{W\text{-}v}/Kit^{W}$ Mice Contain Mainly Sertoli Cells and a Residual Number of Spermatogonial Stem Cells—$Kit^{W\text{-}v}/Kit^{W}$ mice lack the receptor c-kit, which is expressed from the differentiating type A spermatogonia through the pachytene spermatocytes. Without stimulation of c-kit by its ligand, stem cell factor, differentiated type A spermatogonia and subsequent germ cell stages are lost. All other testicular cell types are maintained (25). Light microscopy analysis of semithin Epon sections of seminiferous tubules of $Kit^{W\text{-}v}/Kit^{W}$ mice revealed the complete absence of spermatocytes and spermatids. The atrophic tubules contained mainly Sertoli cells but also a residual undifferentiated type A spermatogonial compartment, in agreement with previous reports (25). Both differentiating spermatogonia and Sertoli cells undergo apoptosis (Fig. 3, *A* and *B* for overview see also supplemental Fig. 1, *A* and *B*).

"Germ Cell-free" Testes ($Kit^{W\text{-}v}/Kit^{W}$ Mice) Lack Polyenoic Sphingolipids—To distinguish which of the testicular GSLs are associated with germ cells (except from residual spermatogonia), sterile germ cell-free $Kit^{W\text{-}v}/Kit^{W}$ and fertile control $Kit^{W\text{-}v}$ mice were analyzed by TLC. The set of neutral FGSLs was lacking and the set of acidic FGSLs was reduced in $Kit^{W\text{-}v}/Kit^{W}$ testes. Bands due to nonfucosylated GSLs such as Forssman lipid, GM3, GM2, GD1a, GT1b, and GQ1b appeared to be not altered or slightly enhanced (Fig. 3*E*). Whereas neutral FGSLs were reported previously to contain almost exclusively VLC-PUFAs, fucosylated gangliosides also contain to a significant degree palmitic acid (C16:0) (9). Therefore, GSLs of mutant and control testes were further compared by electrospray tandem mass spectrometry: signals corresponding to complex VLC-PUFA containing neutral GSLs (IV^2-α-Fuc-GA1, IV^3-α-Gal,IV^2-α-Fuc-GA1, IV^3-α-GalNAc,IV^2-α-Fuc-GA1, and IV^3-α-GalNAcβ3Gal,IV^2-α-Fuc-GA1) and VLC-PUFA gangliosides (IV^3-α-Gal,IV^2-α-Fuc-GM1a, IV^3-α-GalNAc,IV^2-α-Fuc-GM1a, and IV^3-α-GalNAcβ3Gal,-IV^2-α-Fuc-GM1a) were not detectable in $Kit^{W\text{-}v}/Kit^{W}$ testes. Signals corresponding to VLC-PUFA FucGM1 could be detected in control mice after elimination of GD1 signals by prior digestion of the sample with sialidase from *Vibrio cholerae*. These signals were not present in the testis of $Kit^{W\text{-}v}/Kit^{W}$ mice (data not shown). Taking the detection limits into account, signals for the major VLC-PUFA FGSLs, VLC-PUFA IV^2-α-Fuc-GA1 (FucGA1), were reduced in $Kit^{W\text{-}v}/Kit^{W}$ testes to at least 1% as compared with control testes. As the remaining FGSLs, only IV^2-α-Fuc-GM1a (FucGM1) containing a saturated long-chain fatty acid moiety, palmitic acid, could be detected in $Kit^{W\text{-}v}/Kit^{W}$ testes and appeared to be reduced (Fig. 3, *C* and *D*). In adult mice, FucGM1 is localized mainly in spermatogonia but not in differentiating spermatocytes (9). By quantitative HPLC analysis of derivatized GSLs according to Neville *et al.*[6] (20), neutral FGSLs were undetectable, whereas all four fucosylated acidic GSLs (gangliosides) were detectable but were 50–75% lower in $Kit^{W\text{-}v}/Kit^{W}$ testis as compared with controls (Fig. 6, *D* and *E*). The latter represented the fraction with long-chain saturated but not very long-chain polyunsaturated fatty acid moieties. Further quantitative mass spectrometric analysis of GlcCer and the nonglycosylated sphingolipids ceramide and sphingomyelin revealed that the subsets of these sphingolipids that contain VLC-PUFAs were absent from $Kit^{W\text{-}v}/Kit^{W}$ testes (Fig. 3*F*).

The Expression of Cers3 mRNA, Encoding a Dihydroceramide Synthase, Is Lost in Germ Cell-free Testes ($Kit^{W\text{-}v}/Kit^{W\text{-}v}$ Mice)—Fatty acids are transferred to sphingoid bases by a family of (dihydro)ceramide synthases (CerS) encoded by the genes *Cers1–6* formerly known as longevity assurance genes (*Lass*). To find the CerS potentially responsible for the incorporation of VLC-PUFAs into sphingolipids, testicular mRNA levels of all six *Cers* genes were determined in $Kit^{W\text{-}v}/Kit^{W}$ and corresponding control mice by quantitative real time PCR (qRT-PCR). In control mice, the levels of *Cers* mRNAs could be ranked as *Cers3* > *Cers5* and *Cers2* > *Cers6*. *Cers1* and *Cers4* mRNA were barely detectable. In $Kit^{W\text{-}v}/Kit^{W}$ testes, the level of *Cers3* mRNA was over 150-fold decreased, to 0.6% of control value. *Cers5*, *Cers6*, and *Cers2* mRNAs could also be detected in the germ cell-free testes; their levels were 80, 45, and 20% of control values, respectively (Fig. 3*G*). Taking the overall decrease of Cers mRNAs in $Kit^{W\text{-}v}/Kit^{W}$ testes into account, the only significant decrease that could be responsible for the complete loss of VLC-PUFA sphingolipids was that of *Cers3* mRNA.

During the First Wave of Spermatogenesis Polyenoic Sphingolipids Appear Around Postnatal Day 15/16—Having studied the GSL composition of germ cell-free testes (see above) and those of normal testes (with a full germ cell complement), we monitored the expression of VLC-PUFA glycosphingolipids in the testes during the first wave of spermatogenesis. During this phase of development, the germ cell complement of the testes gradually expands from exclusively spermatogonial precursor cells (gonocytes, at postnatal day 6) to the full range of germ cells, including the first spermatozoa (postnatal day 30–35).

[6] By this HPLC analysis, GSLs are detected quantitatively without the need of individual GSL standards. However it does not discriminate ceramide compositions of individual GSLs. For the latter, mass spectrometry was performed.

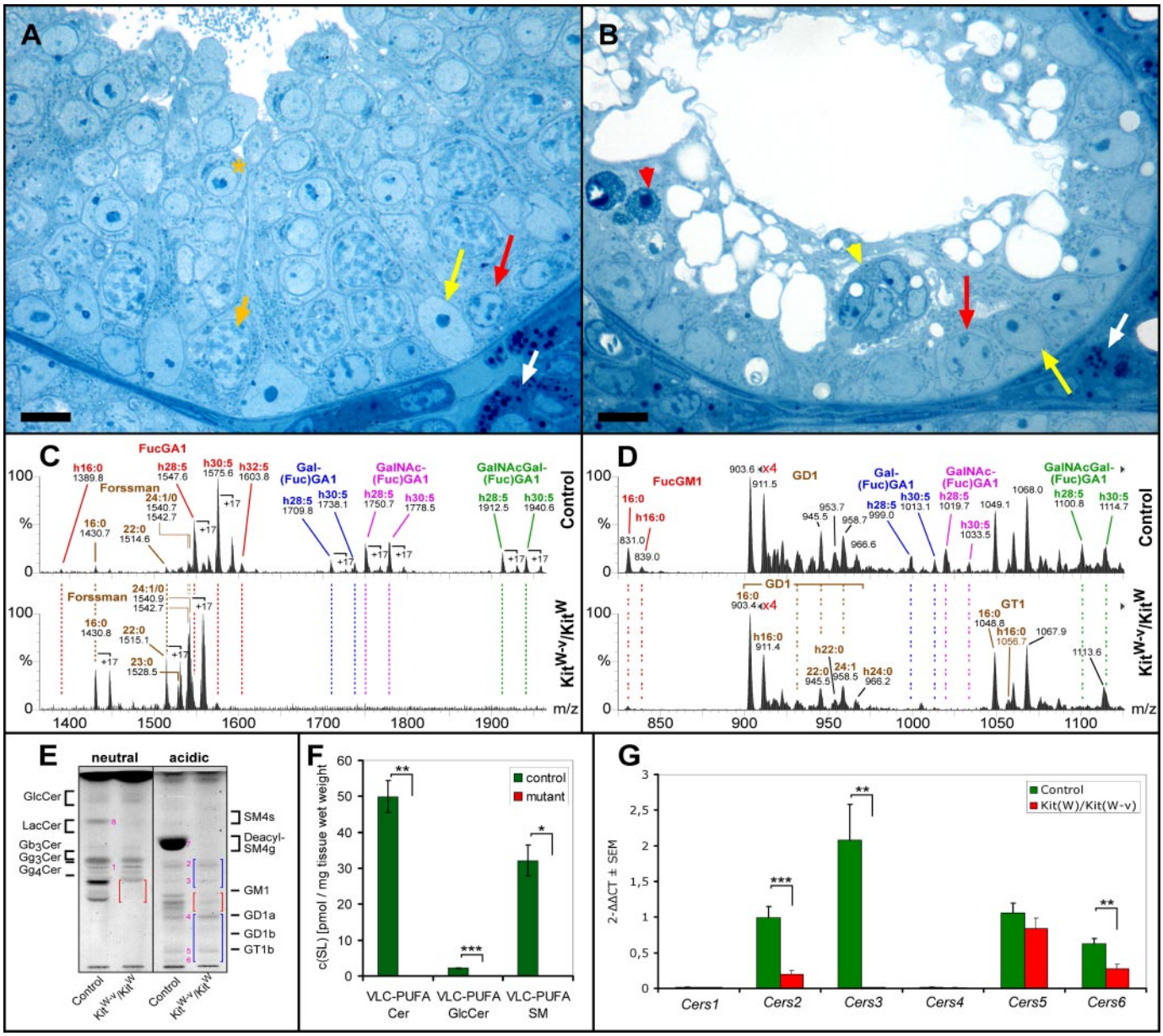

FIGURE 3. **Histological (*A* and *B*), sphingolipid (*C–F*), and *Cers* mRNA (*G*) analysis of testes from 4-week-old control (Kit^{W}) and $Kit^{W\text{-}v}/Kit^{W}$ mice.** *A* and *B*, as compared with controls (*A*), mutant seminiferous tubules (*B*) are atrophic and contain neither intact spermatocytes nor spermatids. A few functional type A spermatogonia (*red arrows*) can be detected along the basement membrane. Note, in mutant mice differentiating spermatogonia undergo apoptosis (*red arrowhead*) as well as Sertoli cells forming multinuclear aggregates (*yellow arrowhead*). Semithin Epon sections were stained with methylene blue-Azur II. *White arrows*, Leydig cells; *yellow arrows*, Sertoli cell nuclei; *short orange arrow*, adluminal primary pachytene spermatocyte; *orange asterisk*, round spermatid; *bar*, 10 μm. *C*, and *D*, nano-electrospray ionization-tandem mass spectrometry characterization of neutral (*C*) and acidic (*D*) complex GSLs from control and $Kit^{W\text{-}v}/Kit^{W}$ (mutant) testis. Complex neutral GSLs were detected with a precursor ion scan of m/z +204. Signals for fucosylated VLC-PUFA GSLs (FucGA1, Gal(Fuc)GA1, GalNAc(Fuc)GA1, and GalNAc-Gal(Fuc)GA1) dominate in control sample with signals of Forssman lipid not exceeding 12% of relative intensity. In mutant ($Kit^{W\text{-}v}/Kit^{W}$) testis, signals for fucosylated VLC-PUFA GSLs are lacking. Signals for Forssman lipid are present and become base peak. Complex gangliosides were detected with a precursor ion scan of m/z −87. Signals for fucosylated VLC-PUFA gangliosides (Gal(Fuc)GM1, GalNAc(Fuc)GM1, and GalNAcGal(Fuc)GM1) are not present in mutant sample, whereas signals for FucGM1(d18:1,16:0), GD1, and GT1 are detected. *E*, TLC of testicular GSLs from control (Kit^{W}) and $Kit^{W\text{-}v}/Kit^{W}$ testes. GSLs were split into a neutral and an acidic fraction and stained after separation with orcinol. *Lanes* correspond to 20 mg of tissue wet weight. *Red* and *blue brackets* denote the migration areas of polyenoic fucosylated GSLs and nonpolyenoic "classical" gangliosides, respectively. Note, bands for neutral polyenoic fucosylated GSLs are not detectable in $Kit^{W\text{-}v}/Kit^{W}$ testes and corresponding bands for acidic polyenoic GSLs are reduced. Bands for Forssman lipid (*band 1*) and nonpolyenoic classical gangliosides GM3 (*band 2*), GM2 (*band 3*), GD1a (*band 4*), GT1b (*band 5*), and GQ1b (*band 6*) appear not to be altered. Seminolipid (*SM4g*) (*band 7*) and its precursor 1-alkyl-2-acyl-3-*O*-β-D-galactosyl-*sn*-glycerol (*GalEAG*) (*band 8*), detected here as deacyl compounds, are also missing in $Kit^{W\text{-}v}/Kit^{W}$ testes. *F*, mass spectrometric quantification of the VLC-PUFA sphingolipids ceramide, GlcCer, and sphingomyelin from control (Kit^{W}) and $Kit^{W\text{-}v}/Kit^{W}$ testes. Internal standards for Cer, GlcCer, and SM were added to lipid extracts. Cer and GlcCer were detected with the precursor ion mode m/z +264 selective for d18:1 and t18:0 sphingoid base containing sphingolipids. SM was detected with the precursor ion mode m/z +184 selective for the phosphorylcholine head group. *G*, quantitative real time-PCR of Cers mRNAs from control (Kit^{W}) and $Kit^{W\text{-}v}/Kit^{W}$ testes. The mRNA was isolated from 4-week-old control (Kit^{W}) and $Kit^{W\text{-}v}/Kit^{W}$ testes, transcribed into cDNA, and subjected to qRT-PCR. ΔCT values (CT(*Cers*)-CT(*GAPDH*)) obtained from qRT-PCR were normalized to ΔCT of control *Cers5* mRNA ($\Delta\Delta CT$). *F* and *G*, Student's *t* test, *, $p < 0.05$; **, $p < 0.01$; ***, $p < 0.001$.

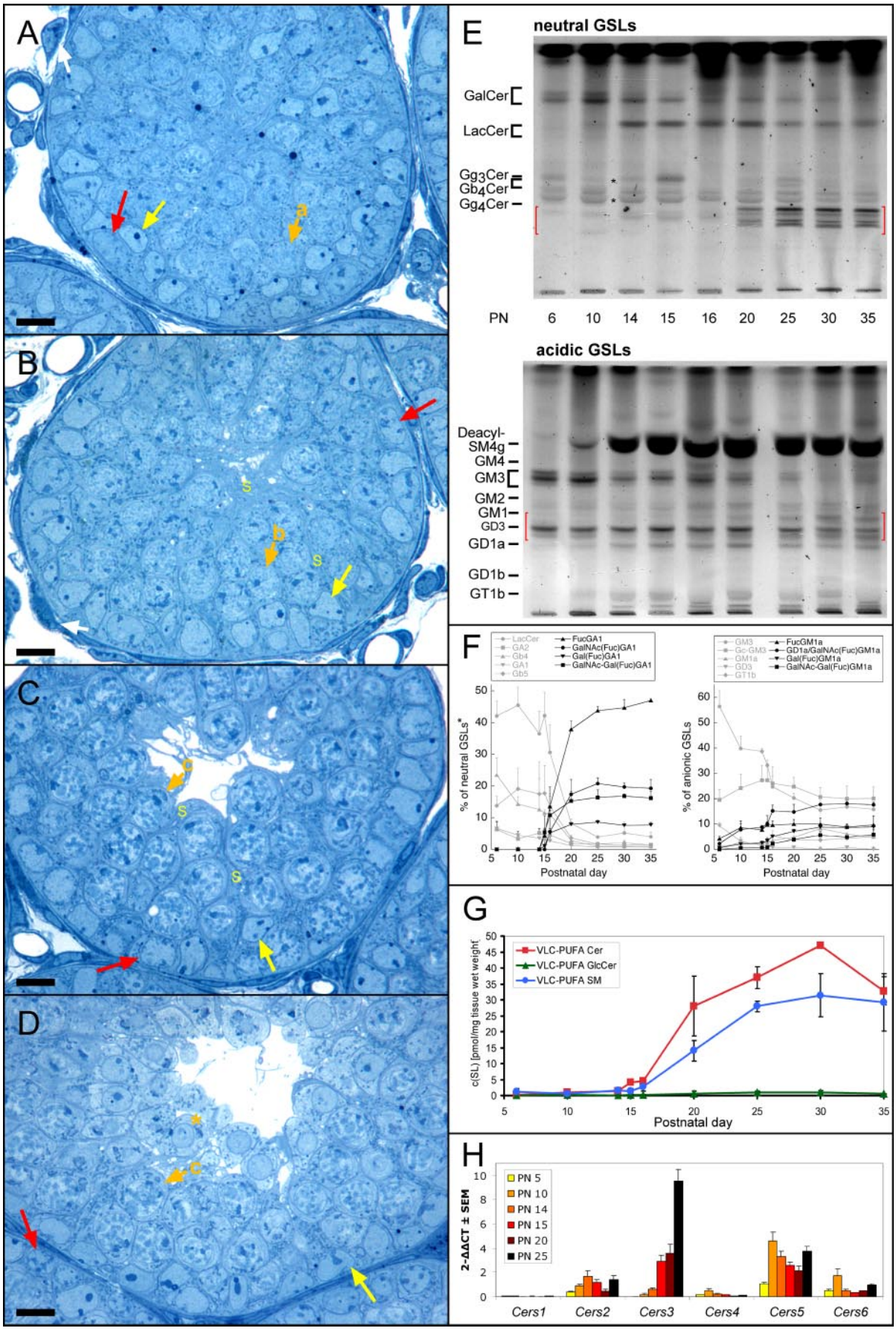
A
B
C
D
E
neutral GSLs
GalCer
LacCer
Gg3Cer
Gb4Cer
Gg4Cer
PN 6 10 14 15 16 20 25 30 35
acidic GSLs
Deacyl-SM4g
GM4
GM3
GM2
GM1
GD3
GD1a
GD1b
GT1b
F
LacCer
GA2
Gb4
GA1
Gb5
FucGA1
GalNAc(Fuc)GA1
Gal(Fuc)GA1
GalNAc-Gal(Fuc)GA1
% of neutral GSLs*
Postnatal day
GM3
Gc-GM3
GM1a
GD3
GT1b
FucGM1a
GD1a/GalNAc(Fuc)GM1a
Gal(Fuc)GM1a
GalNAc-Gal(Fuc)GM1a
% of anionic GSLs
Postnatal day
G
VLC-PUFA Cer
VLC-PUFA GlcCer
VLC-PUFA SM
c(SL) [pmol/mg tissue wet weight]
Postnatal day
H
PN 5
PN 10
PN 14
PN 15
PN 20
PN 25
2-ΔΔCT ± SEM
Cers1
Cers2
Cers3
Cers4
Cers5
Cers6

Over this time the germ cells develop in a synchronized fashion, offering an opportunity to identify at which developmental step germ cells first express the VLC-PUFA sphingolipids. The postnatal germ cell development has been described in detail (26–28). Briefly, seminiferous tubules of newborn mice contain only Sertoli cells and gonocytes, which turn into spermatogonia that subsequently proliferate and differentiate into spermatocytes and spermatids. At 10 days of age meiotic prophase is initiated, and predominantly preleptotene and leptotene primary spermatocytes are visible (Fig. 4*A*, for an overview see supplemental Fig. 2). At P14, spermatocytes of mainly leptotene, zygotene, and pachytene stages are found, and at P15 spermatocytes of pachytene stage are present in most tubules (Fig. 4, *B* and *C*). Between P16 and P18, the functional maturation of Sertoli cells and the blood-testis barrier are established (supplemental Fig. 3). At P20 most seminiferous tubules contain large numbers of pachytene spermatocytes, and some round spermatids are found (Fig. 4*D*). At P30 the number of round spermatids enlarges, and 50% of the tubules also contain elongating spermatids (supplemental Fig. 2).

TLC analysis and HPLC quantification revealed that the subset of neutral FGSLs, essential for spermatogenesis beyond the stage of round spermatids, was absent before day P15 but became the major neutral GSL fraction by P20. The simple gangliosides GM3 and GD3, which are faint or not detectable in adult testis, were strongly expressed before P15. After P10, levels of GM3 and GD3 decreased, changing inversely in relation to the amounts of neutral FGSLs (Fig. 4, *E* and *F*, and supplemental Fig. 4).

The content of VLC-PUFAs in sphingolipids (GSLs, ceramide, and sphingomyelin) was also analyzed by mass spectrometry. All GSLs, including the fucosylated gangliosides, ceramides, and sphingomyelins present before day P15 had long-chain but not very long-chain fatty acid length (C16–C24), and their fatty acids were saturated (C16:0–C24:0) or monounsaturated (C24:1). Palmitic acid was the major fatty acid of sphingolipids before day P15 (supplemental Figs. 5 and 7). Small amounts of VLC-PUFA Cer, VLC-PUFA SM (Fig. 4*G*), and VLC-PUFA GSLs (supplemental Fig. 5) could be detected at P15. Within the next 5 days, VLC-PUFA Cer and SM increased conspicuously. At P20, the VLC-PUFA Cer concentration was at the same level as at P35, whereas VLC-PUFA SM reached a maximum at P25 and remained at this level to P35 (Fig. 4*G*). At the latter time point, the combined concentration of VLC-PUFA Cer and VLC-PUFA SM (30 pmol/mg tissue wet weight) was similar to that of the VLC-PUFA GSLs.

Cers3 Is Up-regulated during Juvenile Testicular Maturation—To establish whether any of the ceramide synthases could be linked to the rise in VLC-PUFA GSLs taking place from day 14/15, levels of *Cers* mRNAs were analyzed by qRT-PCR in testes of P5 to P25 mice. In the early development prior to P15, *Cers5* was the most abundant *Cers* mRNA in testes followed by 2–6 times lower amounts of *Cers2* and *Cers6* mRNA. No significant levels of *Cers4* and *Cers1* mRNAs could be detected. After an initial increase between P5 and P10, *Cers5* mRNA levels stayed roughly constant, similar to *Cers1, -2, -4,* and *-6*. In contrast, *Cers3* mRNA was more than 700-fold upregulated from P5 to P25. Although hardly detectable at P5, significant amounts of *Cers3* mRNA appeared at P14 that 24 h later reached similar levels to *Cers5* mRNA and further increased to 2.5-fold the amount of *Cers5* mRNA at P25 (Fig. 4*H*). Thus, the increase in VLC-PUFA GSLs, taking place from postnatal day 14–25, coincided with a strong elevation of *Cers*3 mRNA.

In Adult Testes, the Levels of Neutral Fucosylated GSLs Correlate with the Progress of Spermatogenesis—To complement the analysis of testicular sphingolipids during postnatal development, we studied testes from mutant and genetically engineered adult mice that have arrests at different steps in spermatogenesis. We have used the testes from *XXSxr^b* and *mshi* mutant mice and from *bax*- and *CREM*-deficient mice. *XXSxr^b* mice have a failure of spermatogonial mitosis. Besides Sertoli cells, their seminiferous tubules contain only early spermatogonia and closely resemble those of *Kit$^{W\text{-}v}$/Kit^W* mice, except that seminiferous tubules of XXSxr^b mice have rare small foci of further germ cell development to the spermatocyte stage (early pachytene) (29). *mshi* mice have reduced numbers of spermatogonia and spermatocytes; the latter fail to complete the meiotic phase (30). *Bax*-deficient mice accumulate atypical premeiotic germ cells, whereas small numbers of germ cells complete meiotic karyokinesis and then remain as multinuclear giant cells containing the nuclei of round spermatids (31). *CREM*-deficient mice display a postmeiotic arrest at the first step of spermiogenesis (32, 33). When ranking this set of testes relative to

FIGURE 4. **Histological (*A–D*), sphingolipid (*E–G*), and Cers mRNA (*H*) analysis of juvenile testes during postnatal development.** *A–D,* postnatal development of the seminiferous epithelium in control mice testes at the ages of P10 (*A*), P14 (*B*), P15 (*C*), and P20 (*D*). Note the stage-specific appearance of late leptotene (*arrow a*), zygotene (*arrow b*), pachytene primary spermatocytes (*arrow c*, *short orange arrows*), and round spermatids (*orange asterisk*) during the first wave of spermatogenesis. Semithin Epon sections were stained with methylene blue-Azur II. *Yellow arrows*, Sertoli cell nuclei; *yellow S*, Sertoli cell processes; *red arrows*, spermatogonia; *bar*, 10 μm. *E,* TLC of testicular GSLs from juvenile and pubertal testes at different stages of testicular development. GSLs were separated into a neutral and an acidic fraction and stained after separation with orcinol. Lanes correspond to 20 mg of tissue wet weight. *Red brackets* denote the migration areas of polyenoic fucosylated GSLs. Note, bands for neutral polyenoic fucosylated GSLs are not detectable before P20. During early stages (P6–14) intensely stained bands for GlcCer, GM3, and GD3 appear. Seminolipid (*SM4g*) is detectable at P10 and is highly expressed from P14 onward. *F,* HPLC quantification of testicular GSLs from juvenile and pubertal testes at different stages of testicular development. GSLs were derivatized and separated by HPLC. Note, neutral fucosylated GSLs increase remarkably between P15 and P25, whereas LacCer and its acidic derivatives GM3 and GD3 decrease significantly between P5 and P20. Other GSLs appear to be unaltered. *, GlcCer levels are not included by this method. For absolute amounts of neutral and acidic GSLs, see supplemental Fig. 4. *G,* mass spectrometric quantification of the polyenoic sphingolipids ceramide, GlcCer, and sphingomyelin. Internal standards for Cer, GlcCer, and SM were added to lipid extracts. Cer and GlcCer were detected with the precursor ion mode m/z +264 selective for d18:1 and d18:0 sphingoid base containing sphingolipids, and SM was detected with the precursor ion mode m/z +184 selective for the phosphorylcholine head group. Note, VLC-PUFA Cer and VLC-PUFA SM increase strongly from P15 onward. The increase of VLC-PUFA SM has a delay as compared with VLC-PUFA Cer, before they finally reach similar levels at P35. *H,* quantitative real time PCR of *Cers* mRNAs from juvenile testes (P5–P25). The mRNA was isolated from prepubertal testes at different points of development, transcribed into cDNA, and subjected to qRT-PCR. *A*, ΔCT values (*CT*(*Cers*)-CT(*GAPDH*)) obtained from qRT-PCR were normalized to ΔCT of *Cers5* mRNA ($\Delta\Delta CT$) at P5. Note, *Cers3* mRNA continuously increases from P5 to P25 with over 700-fold change, whereas *Cers5* mRNA displays already a relatively strong expression before P14.

the extent to which they support spermatogenesis (*XXSxr*^{b} – *Mshi* – *Bax*$^{-/-}$ – *CREM*$^{-/-}$), we observed an increase in the percentage of neutral fucosylated GSLs (Fig. 5*B* and Table 2) and a decrease of neutral nonfucosylated GSLs (Fig. 5*D*). In contrast, the relative levels of gangliosides were not correlated with the progression of spermatogenesis, irrespective of their fucosylation (Fig. 5, *C* and *E*). Thus, also in adult testes the progression of germ cells through meiosis was correlated with high levels of neutral fucosylated GSLs. The GSL profile of the CREM$^{-/-}$ testes was comparable with that of control testes (Fig. 5, *B–E*, and Table 2). The concentration of the corresponding acidic monosialo-FGSLs did not correlate with progressing spermatogenesis, confirming their main presence in spermatogonia (Fig. 5*C* and Table 2) (9).

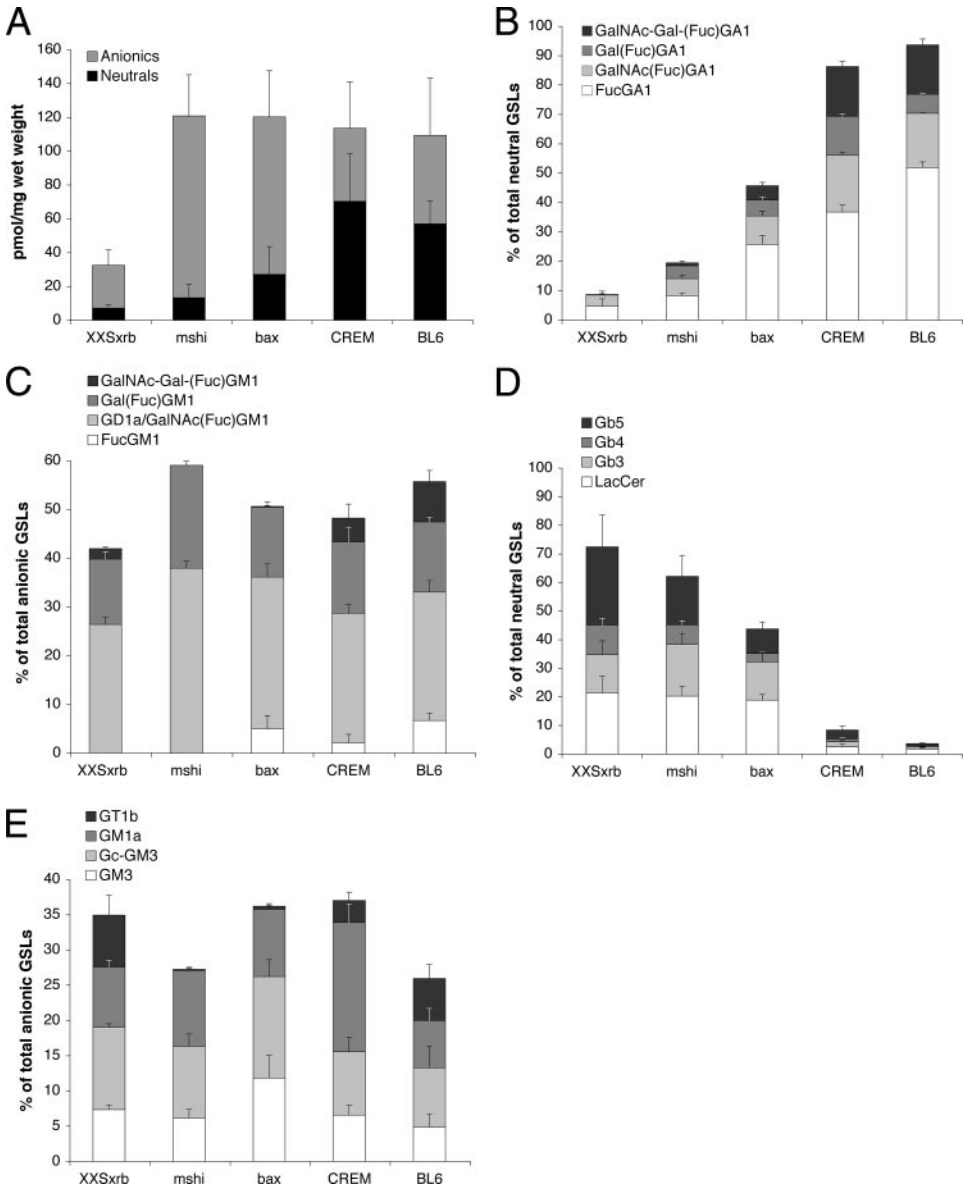

FIGURE 5. **GSL analysis of testis from sterile mutant mice.** Testicular GSLs from *XXsxr*^{b}, *mshi*, *bax*$^{-/-}$, and *CREM*$^{-/-}$ mice were derivatized and separated by HPLC. *A,* total levels of neutral GSLs and gangliosides. *B* and *C,* relative amounts of fucosylated neutral GSLs (*B*), and gangliosides (*C*) with respect to all neutral GSLs or gangliosides, respectively. *D* and *E,* relative amount of nonfucosylated neutral GSLs (*D*) and gangliosides (*E*), with respect to all neutral GSLs or gangliosides, respectively. Note, fucosylated neutral GSLs but not fucosylated gangliosides increase remarkably from *XXsxr*^{b} over *mshi* and *bax*$^{-/-}$ to *CREM*$^{-/-}$ testes, and therefore correlate with the progressing stages of spermatogenesis found in these mice. GlcCer levels are not determined with this method and are not included with the neutral GSLs.

Infertile Galgt1$^{-/-}$ *Mice Lacking Fucosylated Complex Ganglio-series GSLs Still Contain VLC-PUFA Ceramides, Sphingomyelins, and Lactosylceramides*—Sterile GalNAc transferase-deficient (*Galgt1*$^{-/-}$) mice have an arrest in spermatogenesis after adluminal completion of meiotic karyokinesis (Fig. 6, *A* and *B*) and lack complex ganglio-series GLSs, including VLC-PUFA FGSLs (9). To further delineate whether these mice are sterile because of the complete loss of VLC-PUFA sphingolipids, we analyzed the simple sphingolipids Cer, SM, GlcCer, and LacCer in addition to the FGSLs with respect to their acyl chains. As expected from previous TLC and MS data (9), HPLC analysis confirmed the lack of all neutral FGSLs, similar to the germ cell-deficient *Kit*$^{W\text{-}v}$/*Kit*^{W} mice (Fig. 6*D*). However, the *Galgt1*$^{-/-}$ testes were comparable with control (*Galgt1*+/−) testes, in that they contained "simple" VLC-PUFA sphingolipids, albeit in different amounts. They had 60% less VLC-PUFA sphingomyelins and 9 times more VLC-

TABLE 2

Relative amounts of nonfucosylated and fucosylated GSLs in mouse models with arrests at various steps of spermatogenesis

Values are expressed as mean ± S.D.

Mouse model	Spermatogenesis arrest at stage(s)	Neutral GSLs		Anionic GSLs	
		Nonfucosylated	Fucosylated	Nonfucosylated	Fucosylated + GD1a
		%		%	
XXSxr^{b}	Spermatogonia	79.0 ± 6.5	8.7 ± 1.7	34.9 ± 2.0	42.1 ± 2.7
mshi	Spermatogonia/spermatocytes	70.4 ± 2.1	19.5 ± 2.0	27.3 ± 3.2	59.2 ± 2.0
bax$^{-/-}$	Spermatogonia/spermatids	50.3 ± 2.2	45.7 ± 6.4	36.2 ± 5.6	50.7 ± 5.1
CREM$^{-/-}$	Early spermatids	11.6 ± 0.6	86.3 ± 0.9	37.0 ± 4.6	48.3 ± 6.1
C57BL/6	None	05.1 ± 0.7	93.7 ± 0.4	25.9 ± 4.7	55.8 ± 6.8

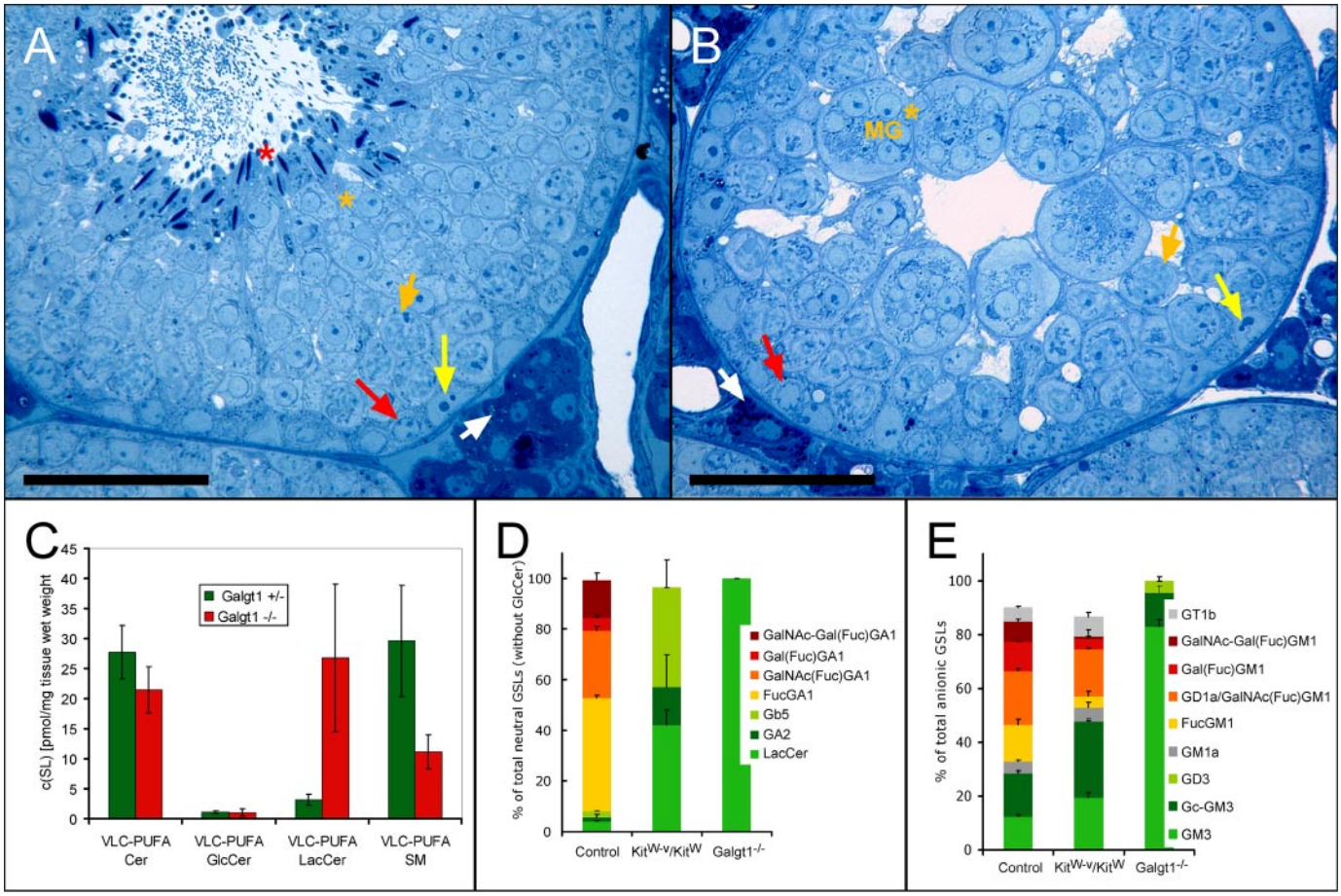

FIGURE 6. **Histological (*A* and *B*) and sphingolipid- (*C–E*) analysis of infertile *Gaglt1*$^{-/-}$ and corresponding control (*Gaglt1*$^{+/-}$) testes.** *A* and *B,* seminiferous tubules of mutant testis (*B*) do not contain maturing spermatozoa (*red asterisk*) as compared with controls (*A*). Note, nuclei of round spermatids (*orange asterisks*) in mutants are almost exclusively found in multinuclear giant cells (*MG*). Semithin Epon sections were stained with methylene blue-Azur II. *White arrows*, Leydig cells; *yellow arrows*, Sertoli cell nuclei; *red arrows*, spermatogonia; *short orange arrows*, adluminal primary pachytene spermatocytes; *bar*, 50 μm. *C,* mass spectrometric quantification of the polyenoic sphingolipids ceramide, GlcCer, LacCer, and sphingomyelin from control (*Gaglt1*$^{+/-}$) and *Gaglt1*$^{-/-}$ testes. Internal standards for Cer, GlcCer, LacCer, and SM were added to lipid extracts. Cer, GlcCer, and LacCer were detected with the precursor ion mode *m/z* +264 selective for d18:1 and d18:0 sphingoid base containing sphingolipids, and SM was detected with the precursor ion mode *m/z* +184 selective for the phosphorylcholine head group. Student's *t* test, *, $p < 0.05$; **, $p < 0.01$; ***, $p < 0.001$. Note, the remarkable increase in VLC-PUFA LacCer compensates for the loss of fucosylated GSLs, and VLC-PUFA SM decreases significantly in *Gaglt1*$^{-/-}$ testis. *D* and *E,* percent relative levels of GSLs of all neutral (*D*), and acidic GSLs (*E*), in *Gaglt1*$^{-/-}$ and *Kit*$^{W\text{-}v}$/*Kit*^{W} testes as compared with controls. Data were obtained on HPLC and thus do not include GlcCer.

PUFA LacCer, the biosynthetic precursor of VLC-PUFA FGSLs. On a molar basis this increase corresponded to the amount of the VLC-PUFA FGSLs that were lacking. No significant changes were found in the composition of VLC-PUFA ceramides and VLC-PUFA GlcCers (Fig. 6*C*).

Fucosylation of Germ Cell GSLs Is Not Essential for Fertility and Spermiogenesis—To investigate the significance of the fucosylation of the neutral VLC-PUFA GSLs, we studied the GSLs from mice lacking the transporter responsible for the import of GDP-fucose into the Golgi (Slc35c1$^{-/-}$). These mice have a profound reduction of fucosylated glycoconjugates in tissues and isolated cells. Although showing severe growth retardation and a shortened life span, male Slc35c1$^{-/-}$ mice are fertile (16). Histological analysis of testes revealed no significant changes in the seminiferous epithelium demonstrating normal spermatogenesis/spermiogenesis (Fig. 7, *A* and *B*). The testes of these mice did not contain any fucosylated GSLs. All eight GSLs that are fucosylated in control testes were expressed in Slc35c1$^{-/-}$ testes without fucosylation, but they still contained VLC-PUFAs to a similar extent as in controls (Fig. 7, *C* and *D*).

DISCUSSION

By elucidating and comparing testicular GSL profiles of infertile *Galgt1*$^{-/-}$ and fertile *Siat9*$^{-/-}$ mutants with control mice, it was previously shown that complex neutral FGSLs containing VLC-PUFAs (more than 24 carbon atoms and 4–6 double bonds) appeared to be essential for spermatogenesis to proceed beyond the formation of round spermatids. Two of the four neutral FGSLs, FucGA1 and GalNacGal(Fuc)GA1, had been linked by immunocytochemistry to adluminal spermatocytes and spermatids. One of the four corresponding acidic FGSLs, FucGM1, was localized in spermatogonia but not in spermatocytes (9). As this class of FGSLs is distinguishable from the other 13 testicular neutral and acidic GSLs by the incorporation of VLC-PUFAs into their ceramide moieties, we suggested that all of them are expressed by germ cells. To test this hypothesis, we investigated testes of *Kit*$^{W\text{-}v}$/*Kit*^{W} mice, lacking differentiating germ cells. The histological analysis revealed that testes of these mice still contain some undifferentiated type A spermatogonia, which upon differentiation

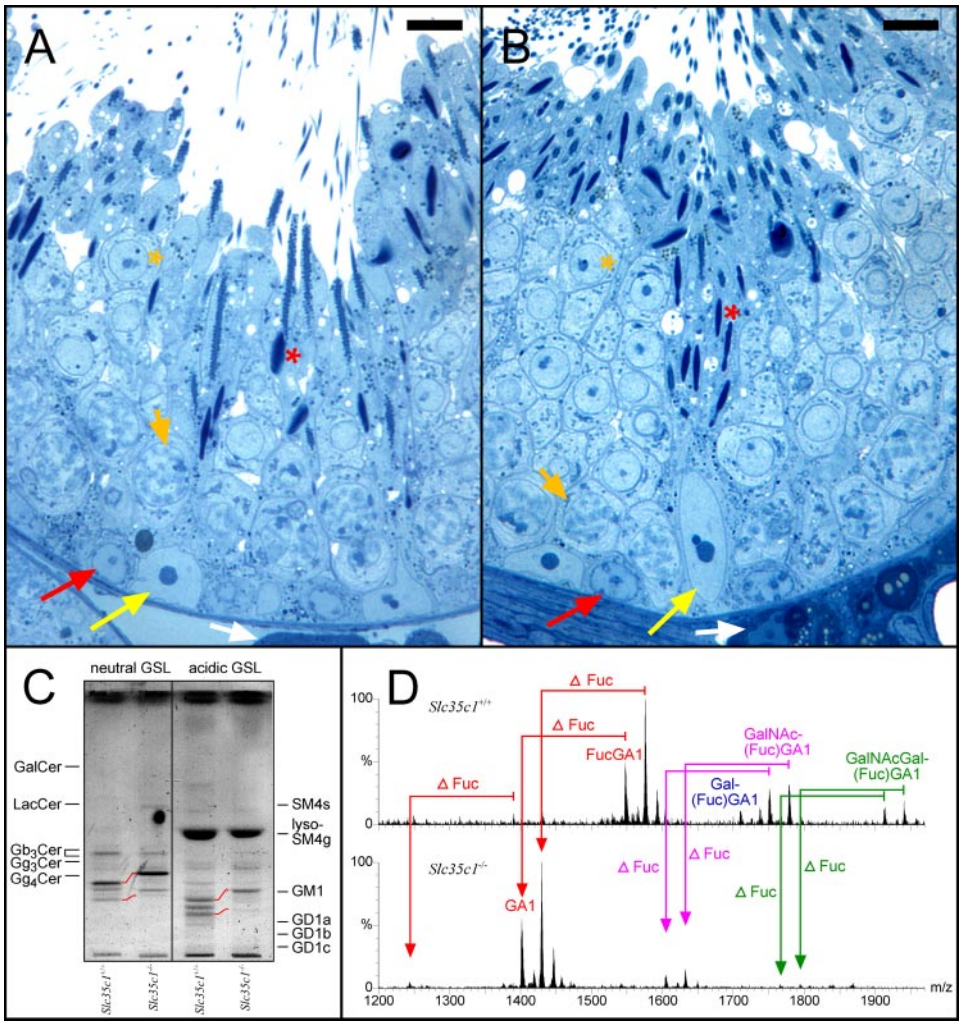

FIGURE 7. **Histological (*A* and *B*) and sphingolipid (*C* and *D*) analysis of fertile *Slc35c1*$^{-/-}$ and corresponding control (*Slc35c1*$^{+/+}$) testes.** *A* and *B*, no significant changes were observed in the architecture of the seminiferous epithelium of mutant mice testes (*B*) as compared with controls (*A*). Note, maturating spermatozoa (*red asterisks*) are present in both control and mutant testis. Semithin Epon sections were stained with methylene blue-Azur II. *White arrows*, Leydig cells; *yellow arrows*, Sertoli cell nuclei; *red arrows*, spermatogonia; *short orange arrows*, adluminal primary pachytene spermatocytes; *orange asterisks*, round spermatids; *bar*, 10 μm. *C*, TLC of testicular GSLs from control (*Slc35c1*$^{+/+}$) and *Slc35c1*$^{-/-}$ testis. GSLs were split into a neutral and an acidic fraction and stained after separation with orcinol. *Lanes* correspond to 20 mg of tissue wet weight. *Red lanes* denote the shift in migration observed for GSLs of mutant mice. Instead of bands for FucGA1 and FucGM1, bands for GA1(Gg_4Cer) GM1 are observed in mutant mice. *D*, characterization of neutral complex GSLs from control (*Slc35c1*$^{+/+}$) and *Slc35c1*$^{-/-}$ testes by nano-electrospray ionization-tandem mass spectrometry. Complex neutral GSLs were detected with a precursor ion scan of *m/z* +204. Signals for fucosylated VLCPUFA-GSLs (FucGA1, Gal(Fuc)GA1, GalNAc-(Fuc)GA1, and GalNAcGal(Fuc)GA1) dominate in control sample. In mutant (*Slc35c1*$^{-/-}$) testis, signals for fucosylated VLCPUFA-GSLs are absent. Instead, corresponding signals for nonfucosylated GSLs appear, as measured by a down shift of 146 atomic mass units.

underwent apoptosis. Therefore, no intact spermatocytes or spermatids were detectable, confirming previous findings (25). Testicular lipid analysis revealed that all neutral GSLs, and a major portion of the acidic fucosylated GSLs, were absent from $Kit^{W\text{-}v}/Kit^{W}$ testes with all other GSLs still remaining. Moreover, no mass spectrometric signal for any kind of GSLs containing VLC-PUFAs could be detected in $Kit^{W\text{-}v}/Kit^{W}$ testes. The mutant testes also lacked VLC-PUFA ceramides and sphingomyelins, which were present at relatively high levels in control testes (ceramide is the precursor of GSLs as well as of sphingomyelin). Thus, taking into account the previous immunohistochemical evidence and the current results, it appears that the expression of fucosylated GSLs is restricted to germ cells. Fucosylated gangliosides with long-chain fatty acids are already present in spermatogonia, whereas both neutral and anionic fucosylated GSLs having VLC-PUFAs emerge later during differentiation. Therefore, our findings indicate that the expression of sphingolipids containing VLC-PUFAs is basically restricted to differentiating germ cells (Fig. 1*B*).

To find out at which stage differentiating germ cells start to synthesize GSLs with VLC-PUFAs, testicular sphingolipids were analyzed at different time points within the first wave of spermatogenesis (postnatal day 6–35). Until 14 days after birth no VLC-PUFA sphingolipids (PUSLs) could be detected, with PUSL traces appearing at 15 days after birth (Cer, SM, and FGSLs). This correlates with the appearance of pachytene spermatocytes and is also about the time point of BTB establishment by functionally maturing Sertoli cells (Fig. 1*B*). The BTB, with its tight junction complexes, creates a distinct milieu for differentiating germ cells to complete meiosis and spermiogenesis in the adluminal compartment of the seminiferous tubules. The adluminal milieu could be a factor promoting the expression of PUSLs. Although PUSLs are increasing during the first wave of spermatogenesis, GlcCer, GM3, and GD3, containing mainly palmitic acid, markedly decrease. The latter GSLs appear to be present in somatic testicular cells, which do not change significantly in cell number during testicular maturation. Thus, the abundance of GlcCer, GM3, and GD3 among testicular cells decreases as the number of germ cells in the testis increases during postnatal development (see supplemental Fig. 2).

While investigating adult mutant and genetically engineered mice with spermatogenesis arrests, we found a direct correlation between the amount of testicular neutral FGSLs and the extent to which spermatogenesis proceeded in these mice. This is in agreement with the generation of fucosylated VLC-PUFA GSLs together with the appearance of pachytene spermatocytes during testicular maturation, and it rules out that somatic testicular cells switch on VLC-PUFA sphingolipid synthesis upon testicular maturation.

Our findings are in agreement with reports on testicular VLC-PUFA ceramides and sphingomyelins obtained from other mammalian species, including rats, as published recently by Furland *et al.* (34, 35). Although their results point to a role of polyenoic ceramides and sphingomyelins in sperm capacitation, our results accentuate the importance of polyenoic GSLs early in spermatogenesis.

In the testes from infertile Galgt1$^{-/-}$ mice, spermatogenesis arrests at the stage of round spermatids that aggregate to form multinuclear giant cells. We show that ceramides, sphingomyelins, GlcCers, and LacCers with VLC-PUFAs are present in the Galgt1$^{-/-}$ testis. VLC-PUFA ceramide and VLC-PUFA GlcCer levels did not differ from control values. Importantly, the sphingolipid metabolism is disturbed in three ways in the testes from the mutant mice. First, all GSLs that are synthesized by GalNAc transferase are absent, including the polyenoic complex glycolipids. Second, levels of VLC-PUFA sphingomyelins were decreased; and third, VLC-PUFA LacCer levels were much higher than in control testes. Taking all these alterations in sphingolipid metabolism in Galgt1$^{-/-}$ testis into account, it is essential to distinguish which of the lipid abnormalities is responsible for the impairment of spermatogenesis in the mutant testes.

In *Galgt1*$^{-/-}$ testis, the changes in VLC-PUFA sphingomyelins and LacCer are unlikely to be the cause of the arrest in spermatogenesis. It is rather more plausible that the lack of neutral VLC-PUFA GSLs with complex glycosylation leads to the impairment of germ cell development. Arguments for this are the following. (i) In DBA2 mice, treatment with *N*-butyldeoxynojirimycin (an inhibitor of the non-lysosomal glucosylceramidase GBA2) leads to a significant reduction of VLC-PUFA sphingomyelins but not to an arrest of spermatogenesis (36). (ii) Sphingomyelin synthase 2 is localized in rat testis with late round and elongating spermatids but not to spermatocytes (37). (iii) During the first wave of spermatogenesis, VLC-PUFA ceramide levels reach adult levels before elongating spermatids are found (P20), whereas VLC-PUFA sphingomyelins reach adult level 5 days later (Fig. 4*G*). (iv) DBA2 mice have very high levels of LacCer in many tissues, including testes,[7] but they are normally fertile.

We also have investigated whether fucosylation of germ cell GSLs is required for spermatogenesis. Investigation of mice lacking the Golgi transporter for GDP-Fuc indicates that this is not the case. These mice express complex VLC-PUFAs GSLs in their testes, simply without fucosylation (*e.g.* GA1 instead of FucGA1 etc.). In addition, these mice appear to have normal spermatogenesis, as judged from the histological analysis of their testes. Furthermore, offspring were successfully obtained from homozygote male and female (*Slc35c1*$^{-/-}$) breeding pairs (16).

Currently, we hypothesize that a combination of the polyenoic ceramide-anchor together with a complex carbohydrate structure, containing at least the GA2-sugar moiety, could be essential for preventing male infertility of *Galgt1*$^{-/-}$ mice. To prove this, analysis of mice with cell type-specific deletions in germ cells of either GSLs or the VLC-PUFA properties of the ceramide-anchor will be necessary.

Understanding PUSL biosynthesis at a molecular level is a prerequisite to address functional studies involving the modulation or deletion of testicular PUSL synthesis. Therefore, we aimed to identify the gene encoding the enzyme responsible for the incorporation of very long-chain polyunsaturated fatty acids into sphingolipids. The condensation of acyl-CoAs with sphinganine (and/or sphingosine) is catalyzed by a family of six (dihydro)ceramide synthases (CerS1–6). *In vitro* studies revealed differential substrate specificities of the six different mouse CerSs. CerS3 has been reported to be specifically expressed in testis on mRNA levels, and the authors found a rather unspecific affinity of CerS3 for acyl-CoAs. Acyl-CoAs investigated ranged in length from C16 to C26 and were all saturated (38). Unsaturated or testis-specific very long-chain polyunsaturated acyl-CoAs ((h)C28–32:4–6) still remain to be added to these investigations.

Using qRT-PCR, we found *Cers2*, *-3*, *-5*, and *-6* mRNAs to be expressed in testis. In adult testis *Cers3* expression was highest followed by *Cers*, whereas in infantile testis (P5–P14) *Cers5* expression was highest. CerS5 and CerS6 (*Cers5* and *-6*) preferentially transfer palmitic acyl to sphingoid bases (39, 40), and CerS2 (*Cers2*) shows a preference for C22/24-chain length acyl-CoAs (40). The mRNA of all these three CerSs are expressed before P14 and do not increase later during testis maturation. Furthermore, Cers2, -5, and -6 mRNAs were the only ones present in germ cell-free testes, which do not express VLC-PUFA sphingolipids. This correlates with sphingolipids containing mainly palmitic acid and some behenic (C22) and lignoceric (C24) acid moieties to be found before P14 and in germ cell-free (*Kit*$^{W\text{-}v}$/*Kit*^{W}) testes. *Cers3* mRNA expression, in contrast to the other *Cers* mRNAs, is lost together with VLC-PUFA sphingolipid expression in mouse testes, which do not contain differentiating germ cells (*Kit*$^{W\text{-}v}$/*Kit*^{W}). Furthermore, *Cers3* is the only *Cers* that is significantly up-regulated between P10 and P20, when PUSLs appear. Therefore, we link testis CerS3 to the synthesis of sphingolipids specifically containing VLC-PUFAs.

Although we could detect minor amounts of VLC-PUFAs (28:5) already at P6 and P10, when no incorporation of these fatty acids into sphingolipids is found, testicular VLC-PUFA levels increase strongly from P15 to P20 in parallel to VLC-PUFA sphingolipid expression (supplemental Fig. 6). The minor amounts found before P15 may be linked to low incorporation into glycerophospholipids, which also at P25 show only minor incorporation of VLC-PUFAs (supplemental Fig. 7). Hence, VLC-PUFA sphingolipid expression in testis probably is a matter of both CerS3 expression and substrate availability. In parallel to the tremendous increase of *Cers3* mRNA around P15, the mRNAs of *Elovl2* and *Elovl5*, encoding two acyl-malonyl-acyltransferases of the "elongation of very long chain fatty acids" family, increase from P10 to P25 by 5–7-fold (supplemental Fig. 8). Each of them alone or both together may be responsible for the enhanced production of VLC-PUFAs in testis. Enhanced VLC-PUFA synthesis may also be supported by roughly a 4-fold higher mRNA expression from P10 to P25 of Δ^6-fatty acid desaturase, which is needed for the desaturation of

[7] D. A. Priestman, unpublished observations.

ω-6 tetracosatetraenic acid ($\Delta^{9,12,15,18}$-24:4) to ω-6 tetracosapentaenic acid ($\Delta^{6,9,12,15,18}$-24:5) (supplemental Fig. 8).

We think it is unlikely that CerS2, -5, or -6, with its mRNAs present at all time stages, synthesize a majority of VLC-PUFA sphingolipids simply because the VLC-PUFA substrates are becoming available; (i) CerS2, -5, or -6 have been characterized to use acyl-CoAs with the length of 16/(18) (CerS5 and -6) or 22/24 carbon atoms (CerS2) in length. If they would in addition have affinity for very long acyl-CoAs (≥28) no matter if saturated, polyunsaturated or hydroxylated, we would assume that they would also have a similar affinity for fatty acids with a length of 26 carbon atoms ((h)26:0–5). But these fatty acids with the length of 26 carbon atoms (26:0, h26:0, 26:4 and 26:5) are not incorporated to a significant degree into sphingolipids, although they are found in relevant amounts (supplemental Fig. 6). (ii) The characterized substrate of CerS2 (40), lignoceric acid (24:0), is not found in fucosylated sphingolipids nor tetracosatetraenic and -pentaenic acid (24:4–5). But these fatty acids (24:0,4–5) are found in testis at all time stages in higher concentrations than the corresponding VLC fatty acids (≥28) (supplemental Fig. 6). So, unless CerS2, -5, and -6 would have a much higher affinity for VLC-PUFA-CoAs than for docosanoic (22:0), tetracosanoic (24:0), or palmitic acid (16:0), respectively, there must be another CerS responsible for VLC-PUFA sphingolipid synthesis, CerS3.

We cannot exclude that, as reported, CerS3 has a "relatively broad substrate specificity" with similar affinities for all acyl-chain lengths. Nevertheless, neutral FGSLs of mouse germ cells contain almost exclusively (hydroxy) very long-chain polyunsaturated fatty acids (C26–C32:4–6), with the two fatty acids h28:5 and h30:5 being prominent. Only minor amounts of neutral FGSLs with palmitic (C16:0) or hydroxypalmitic acid moieties and no FGSLs with fatty acid moieties in the length range of 18 up to 24 carbon atoms were found. At the same time, germ cells contain significant amounts of long-chain saturated fatty acids (C16–C24) (41) and incorporate high amounts of palmitic acid, particularly into seminolipid (42–44). Thus, out of an acyl-CoA pool containing a larger variety of fatty acids, differentiating germ cells incorporate VLC-PUFAs into (G)SLs with high selectivity. As *in vitro* findings not always mirror *in vivo* situations, this selectivity may be achieved by CerS3 itself. The presence of decent amounts of tetracosapentaenic (24:5) and hexacosapentaenic acid (26:5) in testis (supplemental Fig. 6), which are not found to be incorporated to the same degree as VLC-PUFAs into sphingolipids, implies that CerS3 could have a significant affinity for (polyunsaturated) acyl-CoAs with 28 or more carbon atoms but not for (polyunsaturated) acyl-CoAs with 26 or less carbon atoms in length. Alternatively, CerS3 principally could have a broad substrate acceptance, and the specific incorporation observed in testis may be regulated through unknown co-factors, building up a testis-specific enzymatic complex with CerS3.

In conclusion our analytical data indicate that VLC-PUFA GSL with a minimal GA2 core structure are essential for complete spermatogenesis, as we have shown the following. (i) Sterile *Galgt1*$^{-/-}$ mice contain only simple VLC-PUFA sphingolipids (Cer, SM, GlcCer, and LacCer). (ii) Fucosylated GSLs are restricted to germ cells, with their gangliosides expressed mainly in spermatogonia/basal germ cells and their neutral equivalents from the stage of pachytene spermatocytes and beyond. (iii) PUSLs are expressed in differentiating spermatocytes and spermatids from the stage of pachytene spermatocytes. (iv) PUSL expression is regulated by the germ cell stage-dependent expression of the (dihydro)ceramide synthase CerS3. (iv) Fucosylation of germ cell GSLs is not essential for spermatogenesis and fertility.

Currently we suggest that early germ cells, before they pass the blood-testis barrier, synthesize fucosylated gangliosides and simple sphingolipids with long-chain (C16) saturated fatty acid moieties. Passing the BTB and entering the adluminal compartment, differentiating germ cells switch to the production of almost exclusively PUSLs. The production of fucosylated GSLs increases and a relative drop in sialylation activity occurs, thereby leading to mainly neutral FGSLs, which almost exclusively contain VLC-PUFAs. This is corroborated by the increasing mRNA expression of Galgt1, fucosyltransferase 1 and 2, whereas Siat9 mRNA levels stay constant (supplemental Fig. 8).

Thus, the biosynthesis of PUSLs, including complex GSLs, is initiated during the prophase of meiosis I. However, in the final step of meiosis II, after completion of karyokinesis, the clonal spermatid syncytium with its intercellular bridges is not maintained in infertile *Galgt1*$^{-/-}$ mice lacking only the complex GSLs. Thus, we conclude that VLC-PUFA complex GSLs appear to play an essential role in the special membrane processes required for maintenance of intercellular bridges, and/or initiation of spermiogenesis, and establishment of Sertoli cell-spermatid interactions.

Acknowledgments—We thank Ingrid Kuhn-Krause and Mahnaz Bonrouhi for expert technical assistance. We acknowledge Paolo Sassone-Corsi and Paul Burgoyne, who provided testes from CREM$^{-/-}$ *and XXSxr*^{b} *mice, respectively. We are grateful to Britta Brügger for making the triple Quadrupole nanoESI-MS/MS available to us. Pre-experiments for RT-PCR were performed with published primers (45) obtained from Tony Futerman.*

REFERENCES

1. Burgos, M. H., Vitale-Calpe, R., and Aoki, A. (1970) in *The Testis: Development, Anatomy, and Physiology* (Johnson, A. D., Gomes, W. R., and Vandermark, N. L., eds) pp. 551–577, Academic Press, New York
2. Russell, L., Ettlin, R. A., Sinha Hikim, A. P., and Clegg, E. J. (eds) (1990) *Histological and Histopathological Evaluation of the Testis*, pp. 1–38, Cache River Press, Clearwater, FL
3. Russell, L. D. (1980) *Gamete Res.* **3,** 179–202
4. Mruk, D. D., and Cheng, C. Y. (2004) *Endocr. Rev.* **25,** 747–806
5. Fujimoto, H., Tadano-Aritomi, K., Tokumasu, A., Ito, K., Hikita, T., Suzuki, K., and Ishizuka, I. (2000) *J. Biol. Chem.* **275,** 22623–22626
6. Honke, K., Hirahara, Y., Dupree, J., Suzuki, K., Popko, B., Fukushima, K., Fukushima, J., Nagasawa, T., Yoshida, N., Wada, Y., and Taniguchi, N. (2002) *Proc. Natl. Acad. Sci. U. S. A.* **99,** 4227–4232
7. Zhang, Y., Hayashi, Y., Cheng, X., Watanabe, T., Wang, X., Taniguchi, N., and Honke, K. (2005) *Glycobiology* **15,** 649–654
8. Takamiya, K., Yamamoto, A., Furukawa, K., Zhao, J., Fukumoto, S., Yamashiro, S., Okada, M., Haraguchi, M., Shin, M., Kishikawa, M., Shiku, H., and Aizawa, S. (1998) *Proc. Natl. Acad. Sci. U. S. A.* **95,** 12147–12152
9. Sandhoff, R., Geyer, R., Jennemann, R., Paret, C., Kiss, E., Yamashita, T., Gorgas, K., Sijmonsma, T. P., Iwamori, M., Finaz, C., Proia, R. L., Wiegandt, H., and Grone, H. J. (2005) *J. Biol. Chem.* **280,** 27310–27318

10. Kolter, T., and Sandhoff, K. (1999) *Angew. Chem. Int. Ed. Engl.* **38,** 1532–1568
11. Yamashita, T., Hashiramoto, A., Haluzik, M., Mizukami, H., Beck, S., Norton, A., Kono, M., Tsuji, S., Daniotti, J. L., Werth, N., Sandhoff, R., Sandhoff, K., and Proia, R. L. (2003) *Proc. Natl. Acad. Sci. U. S. A.* **100,** 3445–3449
12. Yoon, S. J., Nakayama, K., Hikita, T., Handa, K., and Hakomori, S. I. (2006) *Proc. Natl. Acad. Sci. U. S. A.* **103,** 18987–18991
13. Popko, B. (2000) *Glia* **29,** 149–153
14. Susuki, K., Baba, H., Tohyama, K., Kanai, K., Kuwabara, S., Hirata, K., Furukawa, K., Rasband, M. N., and Yuki, N. (2007) *Glia* **55,** 746–757
15. Liu, Y., Wada, R., Kawai, H., Sango, K., Deng, C., Tai, T., McDonald, M. P., Araujo, K., Crawley, J. N., Bierfreund, U., Sandhoff, K., Suzuki, K., and Proia, R. L. (1999) *J. Clin. Investig.* **103,** 497–505
16. Hellbusch, C. C., Sperandio, M., Frommhold, D., Yakubenia, S., Wild, M. K., Popovici, D., Vestweber, D., Grone, H. J., von Figura, K., Lubke, T., and Korner, C. (2007) *J. Biol. Chem.* **282,** 10762–10772
17. Sandhoff, R., Hepbildikler, S. T., Jennemann, R., Geyer, R., Gieselmann, V., Proia, R. L., Wiegandt, H., and Grone, H. J. (2002) *J. Biol. Chem.* **277,** 20386–20398
18. Jennemann, R., Sandhoff, R., Wang, S., Kiss, E., Gretz, N., Zuliani, C., Martin-Villalba, A., Jager, R., Schorle, H., Kenzelmann, M., Bonrouhi, M., Wiegandt, H., and Grone, H. J. (2005) *Proc. Natl. Acad. Sci. U. S. A.* **102,** 12459–12464
19. Jennemann, R., Sandhoff, R., Langbein, L., Kaden, S., Rothermel, U., Gallala, H., Sandhoff, K., Wiegandt, H., and Grone, H. J. (2007) *J. Biol. Chem.* **282,** 3083–3094
20. Neville, D. C., Coquard, V., Priestman, D. A., te Vruchte, D. J., Sillence, D. J., Dwek, R. A., Platt, F. M., and Butters, T. D. (2004) *Anal. Biochem.* **331,** 275–282
21. Gorgas, K., and Krisans, S. K. (1989) *J. Lipid Res.* **30,** 1859–1875
22. Chomczynski, P., and Sacchi, N. (1987) *Anal. Biochem.* **162,** 156–159
23. Adams, J., Kiss, E., Arroyo, A. B., Bonrouhi, M., Sun, Q., Li, Z., Gretz, N., Schnitger, A., Zouboulis, C. C., Wiesel, M., Wagner, J., Nelson, P. J., and Grone, H. J. (2005) *Am. J. Pathol.* **167,** 285–298
24. Livak, K. J., and Schmittgen, T. D. (2001) *Methods* (*San Diego*) **25,** 402–408
25. Ohta, H., Yomogida, K., Dohmae, K., and Nishimune, Y. (2000) *Development* (*Camb.*) **127,** 2125–2131
26. Oakberg, E. F. (1956) *Am. J. Anat.* **99,** 507–516
27. Nebel, B. R., Amarose, A. P., and Hacket, E. M. (1961) *Science* **134,** 832–833
28. Bellve, A. R., Cavicchia, J. C., Millette, C. F., O'Brien, D. A., Bhatnagar, Y. M., and Dym, M. (1977) *J. Cell Biol.* **74,** 68–85
29. Sutcliffe, M. J., and Burgoyne, P. S. (1989) *Development* (*Camb.*) **107,** 373–380
30. Ward-Bailey, P. F., Johnson, K. R., Handel, M. A., Harris, B. S., and Davisson, M. T. (1996) *Mamm. Genome* **7,** 793–797
31. Knudson, C. M., Tung, K. S., Tourtellotte, W. G., Brown, G. A., and Korsmeyer, S. J. (1995) *Science* **270,** 96–99
32. Nantel, F., Monaco, L., Foulkes, N. S., Masquilier, D., LeMeur, M., Henriksen, K., Dierich, A., Parvinen, M., and Sassone-Corsi, P. (1996) *Nature* **380,** 159–162
33. Blendy, J. A., Kaestner, K. H., Weinbauer, G. F., Nieschlag, E., and Schutz, G. (1996) *Nature* **380,** 162–165
34. Furland, N. E., Oresti, G. M., Antollini, S. S., Venturino, A., Maldonado, E. N., and Aveldano, M. I. (2007) *J. Biol. Chem.* **282,** 18151–18161
35. Furland, N. E., Zanetti, S. R., Oresti, G. M., Maldonado, E. N., and Aveldano, M. I. (2007) *J. Biol. Chem.* **282,** 18141–18150
36. Walden, C. M., Sandhoff, R., Chuang, C. C., Yildiz, Y., Butters, T. D., Dwek, R. A., Platt, F. M., and van der Spoel, A. C. (2007) *J. Biol. Chem.* **282,** 32655–32664
37. Lee, N. P., Mruk, D. D., Xia, W., and Cheng, C. Y. (2007) *J. Endocrinol.* **192,** 17–32
38. Mizutani, Y., Kihara, A., and Igarashi, Y. (2006) *Biochem. J.* **398,** 531–538
39. Lahiri, S., and Futerman, A. H. (2005) *J. Biol. Chem.* **280,** 33735–33738
40. Mizutani, Y., Kihara, A., and Igarashi, Y. (2005) *Biochem. J.* **390,** 263–271
41. Grogan, W. M., and Lam, J. W. (1982) *Lipids* **17,** 604–611
42. Ishizuka, I., Suzuki, M., and Yamakawa, T. (1973) *J. Biochem.* (*Tokyo*) **73,** 77–87
43. Suzuki, A., Ishizuka, I., Ueta, N., and Yamakawa, T. (1973) *Jpn. J. Exp. Med.* **43,** 435–442
44. Ishizuka, I. (1997) *Prog. Lipid Res.* **36,** 245–319
45. Riebeling, C., Allegood, J. C., Wang, E., Merrill, A. H., Jr., and Futerman, A. H. (2003) *J. Biol. Chem.* **278,** 43452–43459
46. Svennerholm, L. (1994) *Prog. Brain Res.* **101,** XI–XIV